CrossMark

ORIGINAL PAPER

Waterborne acrylic–polyaniline nanocomposite as antistatic coating: preparation and characterization

Abdolreza Mirmohseni[1] · Ali Gharieh[1] · Manouchehr Khorasani[2]

Abstract An antistatic and electrically conductive acrylic–polyaniline nanocomposite coating was successfully synthesized by interfacial polymerization of aniline in the presence of acrylic latex. The acrylic latex was prepared through emulsion polymerization, and aniline was polymerized by in situ interfacial polymerization at the interface of acrylic latex/chloroform phase. Fourier transform infrared spectroscopy (FTIR), UV–Vis spectroscopy and CHNS elemental analysis revealed the existence of 6.24 wt% emeraldine salt of polyaniline (PAni) in the dried film of the nanocomposite. Scanning electron microscopy (SEM) confirmed the presence of colloidal polymer particles in the aqueous phase which was confirmed to have some advantages, including prevention of aggregation of particles, dispersibility improvement and enhancement of the PAni nanofibers aspect ratio in the acrylic polymer matrix. According to SEM results, PAni fibers with the length ranging from 12 to 67 μm and diameters between 0.078 and 1 μm, highly dispersed in the acrylic polymer matrix, were successfully synthesized. Thermal, electrical and mechanical properties of the acrylic copolymer were significantly affected by PAni incorporation. The onset degradation temperature in thermogravimetric analysis revealed that the thermal stability of the nanocomposite was improved compared to that of the pure acrylic copolymer. The nanocomposite film showed electrical conductivity of about 0.025 S/cm at room temperature, along with satisfactory mechanical properties, attractive as an antistatic material in coating applications.

Keywords Antistatic · Polyaniline · Acrylic · Interfacial polymerization · Emulsion polymerization

Introduction

Nowadays, waterborne acrylic resins are widely used in coating industries as a result of their wide range of excellent properties, including environmentally friendly characteristics and UV–Vis and chemical degradation resistance [1]. However, high electrical insulation properties of these coatings stimulate surface contamination by dust through attraction of static electricity [2]. Also, static charge buildup on such coatings can create the state of sparkling, which may be seriously hazardous in the presence of flammable materials [3].

Antistatic organic coatings are very useful in numerous applications such as electrostatic painting [4], antistatic shielding [5] and polarization filter [6]. The methods of applying metal (oxide)s, carbon and conducting polymers (CPs) in organic coating formulations are known to be useful ways to suppress electrostatic charging [2]. Among the antistatic agents, CPs are known to be potentially efficient materials with advantages in comparison to other methods, including their long-term stability, flame-retardant properties and thermal stability [7]. Among CPs, polyaniline (PAni) [8], with the longest history of applications in various areas of coating industry, is anticorrosive [9, 10] and imparts electromagnetic shielding [11] and antistatic [5] properties. However, one of the major disadvantages of PAni is its hard processability due to its rigid-rod

✉ Abdolreza Mirmohseni
mirmohseni@tabrizu.ac.ir

1 Department of Applied Chemistry, Faculty of Chemistry, University of Tabriz, Tabriz, Iran

2 Department of Polymer Engineering and Color Technology, Amirkabir University of Technology Tehran Polytechnic, Tehran, Iran

IPPI 🖄 Springer

molecular chains. To compensate for this drawback, a variety of polymeric materials with excellent processability (such as epoxy [10] and polyurethane [12]) have been used to prepare PAni composites. These composites could combine the desired properties of the two employed components, i.e., electrical conductivity of PAni with processability and physical–mechanical properties of the polymer matrix [10].

In recent years, due to the growing demand to replace the solvent-borne systems with the waterborne formulations, there have been an increasing volume of literature references based on composites of different CPs, especially PAni and various polymer latexes, such as polyurethane [12], polystyrene [13] and styrene–acrylic copolymers [14, 15]. Mixing of a prepared PAni or polymerization by chemical oxidation in the presence of polymer latexes is the most common technique to achieve waterborne PAni composites. However, a high amount of aggregated PAni and difficulties encountered by highly controlled polymerization conditions are limitations in the above-mentioned preparation methods [16, 17].

The present study reports a feasible and new method for preparing a waterborne conducting composite which consists of colloidal acrylic particles and a conducting polymer such as PAni, in an application such as antistatic coating. For the first time, interfacial polymerization of aniline was employed in in situ synthesis of PAni in the presence of acrylic latex. Through such a process, PAni assembled exclusively in the acrylic latex and a homogenous acrylic–polyaniline (AcPA) nanocomposite could be obtained by a simple practical method.

Experimental

Materials

The monomers, aniline and methyl methacrylate (MMA), were both acquired from Merck Chemical Co.; butyl acrylate (BA) from Fluka and acrylic acid (AA) from BASF were purchased and distilled prior to use. Triton X-100, hydrochloric acid (HCl) and chloroform from Aldrich, and ammonium persulfate (APS) from Merck Chemical Co. were used without any further purification. De-ionized water was used in all recipes.

Procedures

Latex preparation

To prepare acrylic latex with 25 wt% solid content, batch emulsion polymerization was performed in a round-bottomed glass reactor, equipped with a reflux condenser,

mechanical stirrer and nitrogen gas inlet. In a typical procedure, 12 g MMA, 11 g BA, 1 g AA, 70 mL water and 0.9 g Triton X-100 were charged into the reactor. It was mechanically stirred (300 rpm) and after reaching the desired temperature (75 °C), 0.06 g APS, as initiator, was dissolved in 5 mL distilled water and added into the reactor. The polymerization was continued for 3 h with stirring until 98% conversion was reached. The prepared latex was dialyzed thoroughly in dialysis tubes (Medicell International Ltd., MWCO 12–14,000 Da) against phosphate-buffered saline (PBS, pH 7.4) which was replaced every 12 h in the course of over 60 h to eliminate excess surfactants, unreacted monomers and short polymeric chains. The dialysis process was continued until the conductivity of the water outside the dialysis bag remained below 10 $\mu S\ cm^{-1}$. The conductivity was evaluated by two platinum electrodes and an auto-balancing KONDUX Wheatstone bridge (Kamphausen) operating at 380 Hz.

Interfacial polymerization of aniline

Interfacial polymerization of aniline was employed for in situ synthesis of PAni nanofibers [19]. The synthesis procedure is briefly described here. First, a 4.8 mmol of aniline was dissolved in 30 mL chloroform as the organic phase. Then, an aqueous phase which consisted of 0.2 mL HCl 37 wt% and 1.2 mmol APS, dissolved in 30 mL of synthesized latex, was prepared. The organic solution was transferred into a 100 mL container and the aqueous solution was dropwise added during 20 min. The reaction was performed at 25 °C for 140 min.

Characterization

The FTIR spectrum was recorded on a BRUKER-IFS 48 FTIR spectrophotometer (Germany) using the KBr pellet. Optical absorbance in the wavelength range of 300–1100 nm was determined by a Shimadzu UV–Vis spectrophotometer (model UV-2401 PC, Japan). The morphology of the prepared nanocomposite was investigated by a Tescan scanning electron microscope (Vega II instrument, Czech Republic). A drop of each prepared sample was placed on the sample holder and dried. All were then put under vacuum, flushed with argon (Ar), evacuated and sputter-coated with gold for SEM analysis. A homemade four-point probe was used to measure the DC electrical conductivity of the AcPA nanocomposite. The free-standing films of nanocomposites with the dimensions of 20 × 7 × 0.3 cm were used for the measurement of electrical conductivity. The electrical conductivity values were reported as averages of at least five individual measurements recorded from different places of the prepared AcPA
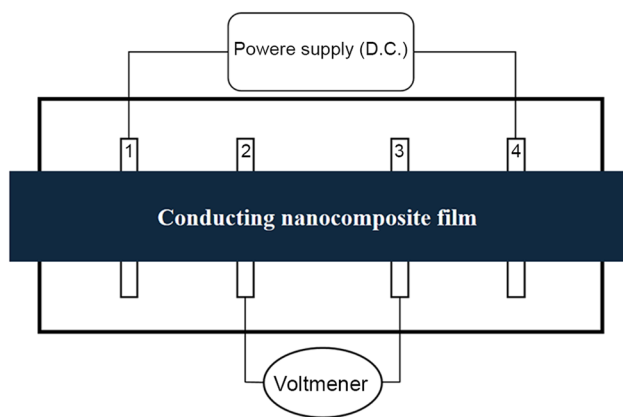
Fig. 1 Scheme of the homemade four-point probe for the measurement of electrical conductivity. *1*, *4*: outer electrodes and *2*, *3*: inner electrodes (objects are not to scale)

film. A schematic configuration of the four-point probe is shown in Fig. 1.

A constant electrical current (16 mA) was applied between two opposite inner electrodes and the voltage (ΔE) was recorded between two other opposed electrodes. The electrical conductivity (S cm^{-1}) was calculated using Eq. (1) [19]:

$$\sigma = 1/R = \frac{Z.Y}{X.I.\Delta E} \tag{1}$$

where *X*, *Y* and *Z* are the nanocomposite film thickness (0.3 cm), center-to-center distance between two opposite electrodes of electrical current (7.15 cm) and distance between two other opposite collectors (2.65 cm), in the order given. ΔE and *I* are the measured potential value (mV) between the two opposite electrodes and the applied current between two other electrodes, respectively. *R* is the electrical resistance (Ω cm) and σ is the electrical conductivity (S cm^{-1}) of the nanocomposite film. Because of low electrical conductivity, a two-point measurement method was used to obtain the electrical conductivity of the acrylic film. Elemental analysis was performed by the elemental analyzer (CHNS) Vario ELIII from Elementar Co. (Germany). The mechanical properties of the films were characterized with an Instron 5800 tensile tester at room temperature on dumbbell-shaped specimens cut from the films (thickness of about 0.2 mm). The initial grip distance was 15 mm and the cross-head speed was 2 mm min^{-1}. The measured values were reported as averages of at least five individual measurements. The thermal stability of the prepared nanocomposite was evaluated using a thermogravimetric analyzer. TGA thermographs were recorded on an STA-PL instrument from England. The samples were dried at 60 °C under low-pressure oven until a constant weight was obtained. The dried samples were heated from 50 to 700 °C at a heating rate of 10 °C/min under a nitrogen atmosphere.

Results and discussion

Preparation of AcPA nanocomposite

Poly(methyl methacrylate-*co*-butyl acrylate-*co*-acrylic acid), [poly(MMA-BA-AA)], latex was prepared by emulsion polymerization, followed by incorporation of PAni nanofibers into the latex by interfacial oxidative polymerization. To facilitate film formation of waterborne nanocomposites at room temperature, the glass transition temperature (T_g) of acrylic latex was adjusted around 9 °C by appropriate monomer ratios (BA:MMA:AA) according to the Fox equation (Eq. 2) [20]:

$$\frac{1}{T_{g\,copolymer}} = \frac{w_{MMA}}{T_{g\,MMA}} + \frac{w_{BA}}{T_{BA}} + \frac{w_{AA}}{T_{AA}}, \tag{2}$$

where $T_{g\,copolymer}$ is the glass transition temperature of poly(MMA-BA-AA) and w_{MMA}, w_{BA} and w_{AA} are the weight fractions of MMA, BA and AA in the monomer mixture composition, respectively. Also, $T_{g\,MMA}$, $T_{g\,BA}$ and $T_{g\,AA}$ are glass transition temperatures of the homopolymers. $T_{g\,copolymer}$ was controlled mainly by the MMA:BA ratio. With respect to the Fox equation, it is obvious that by increasing the weight fraction of BA ($T_g = -54$ °C), (or decreasing the weight fraction of MMA, $T_g = 105$ °C), a copolymer is obtained at lower T_g. Acrylic acid, due to its low weight fraction ($w_{AA} = 0.042$), does not show a significant effect on the $T_{g\,copolymer}$, though it can introduce acid functional groups, i.e., carboxyl groups, which exhibit enhanced latex stability and adhesion onto the substrates [21].

Interfacial polymerization was performed at the aqueous/organic biphasic system where oxidizing agent (APS) and dopant (HCl) were dissolved in waterborne acrylic latex (aqueous phase) and aniline was dissolved in chloroform (organic phase). The shape and aspect ratio of PAni nanofibers obtained by interfacial polymerization were not affected by the organic solvent used [17]. Therefore, due to safety considerations, chloroform as a less toxic organic solvent and denser than water was chosen as the organic phase. On the other hand, the diameter of the synthesized PAni nanofibers was affected by the dopants used in interfacial polymerization. Here, to achieve PAni nanofibers with high aspect ratio, HCl was selected among many other doping agents, such as phosphoric, acetic, formic, tartaric, methylsulfonic, ethylsulfonic, camphorsulfonic and 4-toluenesulfonic acid [18].

Aniline polymerization started simultaneously with the formation of interface between the aqueous and organic phases. Figure 2 displays the diffusion of PAni nanofibers

Fig. 2 *Snapshots* showing the formation and migration of PAni during interfacial polymerization
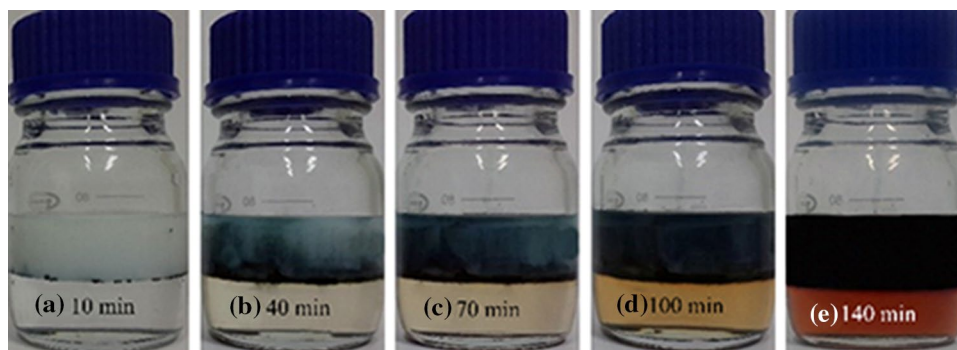
starting from the boundary between the organic and aqueous phases within a few minutes. Green PAni appears at the interface (Fig. 1a), migrates into the aqueous phase (Fig. 1b–d) and finally fills the upper phase (Fig. 1e).

The diffusion rate of PAni nanofibers into the aqueous phase, indicated by changing of the color of the upper phase, is much slower than the rate of conventional interfacial polymerization of aniline (aniline interfacial polymerization in the absence of colloidal particles of latex) [22]. This prolonged interfacial polymerization is probably due to the presence of polymer colloidal particles that behave as physical barriers against the free growth of PAni nanofibers in the aqueous phase.
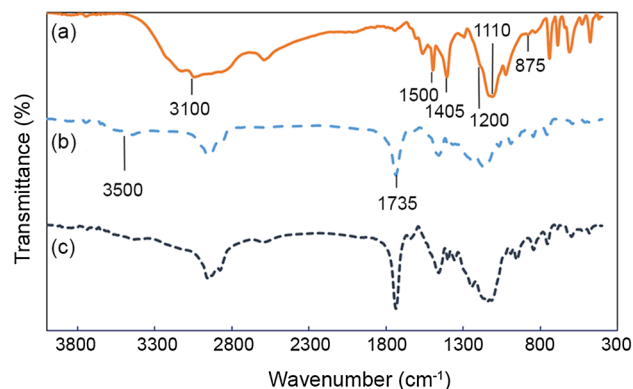
Characterization of AcPA nanocomposites

As can be seen in Fig. 2, the dark green color of the upper phase indicates that PAni in the nanocomposite structure is in its doped state [22]. However, the oxidation state and the formation of polaron band were identified by UV–Vis spectroscopy. As shown in Fig. 3a, the acrylic polymer is almost transparent in the wavelength region 300–1100 nm, while three characteristic absorption peaks are clearly observed in the UV–Vis spectrum of the AcPA nanocomposite, at around 355, 430 and 850 nm (Fig. 3b). The absorption peak appearing at around 355 nm can be ascribed to the π–π* transition of the benzenoid rings, while the peaks appearing at around 430 and 850 nm can be attributed to the polaron–π* and π–polaron transitions, respectively [23]. The spectrum of AcPA nanocomposite indicates that PAni remains in its doped state.

The FTIR spectra of PAni, acrylic copolymer and AcPA nanocomposite samples are shown in Fig. 4. For PAni (Fig. 4a), the bonds at 1405 and 1500 cm^{-1} can be attributed to stretching vibration of the quinonoid and benzenoid rings, respectively. The peak at 1220 cm^{-1} is the characteristic of conducting the protonated form of PAni [24]. The peaks at 1110 and 875 cm^{-1} are related to the aromatic C–H in-plane and out of plane bending of the 1,4-disubstituted aromatic ring, respectively. The broad bond of secondary amine appeared at 3100 cm^{-1}. For acrylic
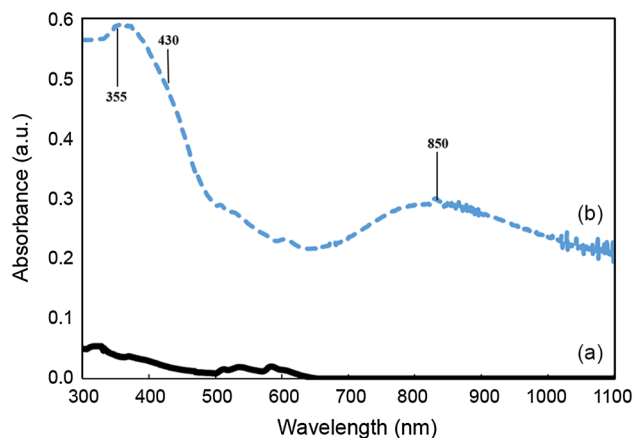

Fig. 3 UV–Vis spectra of **a** the the acrylic copolymer and **b** the AcPA nanocomposite

Fig. 4 FTIR spectra of **a** PAni, **b** acrylic copolymer and **c** AcPA nanocomposite

copolymer (Fig. 4b), the characteristic peak at 1735 cm^{-1} is assigned to the carbonyl stretching vibration. Also, the peaks around 3500 cm^{-1} were related to the –OH symmetric stretching vibrations of the carboxyl group. Figure 4c shows the spectra of the AcPA nanocomposite. The characteristic bonds of both PAni and acrylic copolymer were observed in the spectrum of the prepared nanocomposite.
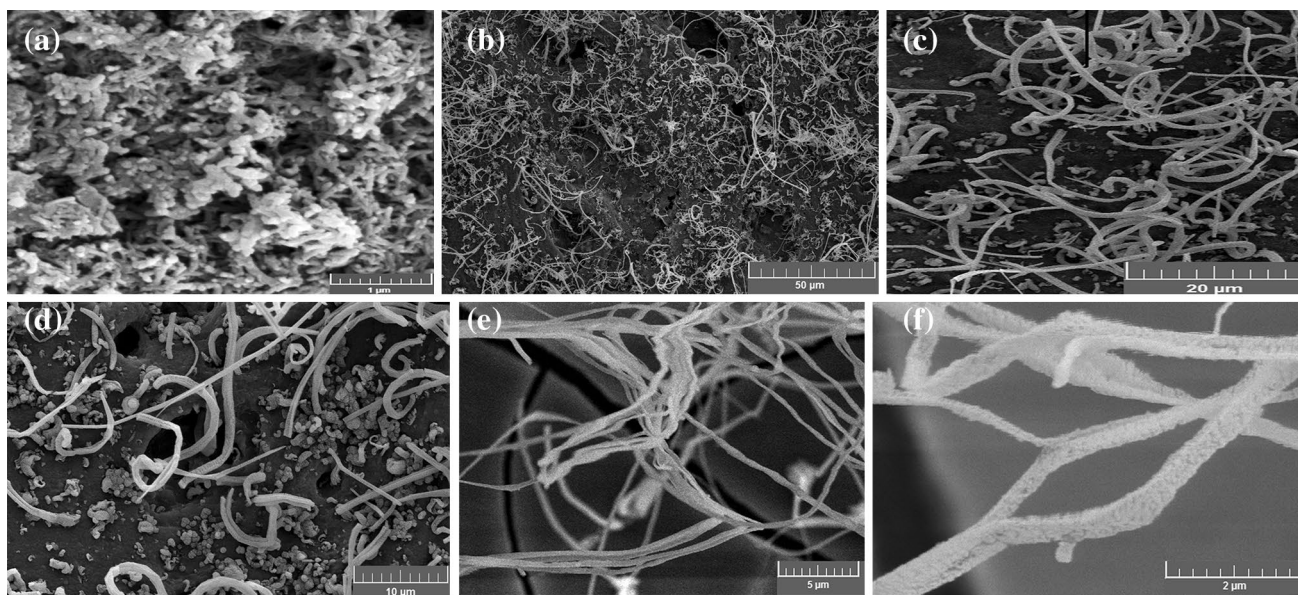
Fig. 5 SEM microstructures of **a** PAni and **b–f** AcPA nanocomposite

The PAni content of the prepared PAAc nanocomposite (excluding the dopant present in the PAni composition) was calculated from the ratio of nitrogen to carbon (N/C) obtained from CHNS analysis [25]. The empirical formula of PAni and acrylic copolymer can be represented as $[(C_6H_4NH) (HCl)]_m$ and $[(MMA)_a (BA)_b (AA)_c]_n$, respectively. The weight fraction of PAni (M) in the nanocomposite was calculated by substituting the experimental N/C values in the following equation:

$$\text{N}/\text{C} = \frac{M\left(\frac{14}{90}\right)}{M\left(\frac{72}{90}\right) + (1-M)\left[\left(\frac{60}{1\square0}\right) + \left(\frac{84}{128}\right) + \left(\frac{36}{72}\right)\right]}. \quad (3)$$

The result of CHNS analysis indicated that interfacial polymerization during 140 min could incorporate 6.24 wt% PAni in the composition of the nanocomposite.

Morphology of the AcPA nanocomposite

Aniline interfacial polymerization is known to be a feasible method to obtain aniline nanofibers and their nanocomposites [26, 27]. PAni nanofibers prepared by this method showed the length of only up to 1 μm [28, 29]. However, it was demonstrated that employing chemical compounds such as *p*-phenylenediamine in interfacial polymerization of aniline could increase the length of PAni nanofibers up to 10 μm [29].

The microstructures of neat PAni nanofibers, prepared by conventional interfacial polymerization, and AcPA nanocomposite were studied by scanning electron microscopy (Fig. 5). As shown in Fig. 5a, conventional interfacial polymerization of aniline results in a large quantity of interconnected nanofibers and nanoparticle aggregates. Dimensions of the prepared PAni nanofibers were analyzed using the ImageJ software. The results indicated that the diameter and length of PAni nanofibers, obtained by conventional interfacial polymerization, were in the range of 25–78 and 0.3–0.8 μm, respectively. On the other hand, PAni nanofibers in the nanocomposite (Fig. 5b–d) show much less entangled and aggregated structures. The length of these PAni nanofibers (~12–67 μm) is higher than the length of any of the PAni nanofibers that have been fabricated by interfacial polymerization technique so far [26–30].

Also, it is clearly obvious that the diameter of the PAni fibers in the nanocomposite structure is in the range of 0.078–1 μm, which is much thicker than the diameters of PAni nanofibers that are obtained by conventional interfacial polymerization (25–78 nm). A possible explanation for this difference might be that, in our experiment, during interfacial polymerization, PAni nanofibers are closer together due to adjacent colloidal particles of latex which surround them. By closing and joining the nanofibers to each other, the diameter of nanofibers increases. This finding which is in agreement with Fig. 5e, f reveals that several PAni nanofibers join together to make thicker fibers.

Briefly, according to the obtained SEM images it could be demonstrated that the presence of colloidal polymer particles altered the morphology of PAni in the AcPA nanocomposite structure from an entangled (nano) fiber

mat to a longer and less entangled nanofiber. In other words, such a synthesis method (i.e., interfacial polymerization of aniline in the presence of colloidal latex particles in aqueous phase) is an efficient technique to prepare conducting composites with embedded ultralong PAni nanofibers.

## Physico-mechanical properties of the AcPA nanocomposite film

PAni incorporation into the acrylic copolymer matrix significantly affected the physical and mechanical properties of the resulting nanocomposite film. The results of room temperature electrical conductivity revealed that the conductivity of the AcPA nanocomposite was several orders of magnitude higher than that of the acrylic latex film. For the nanocomposite, the electrical conductivity was 2.5×10^{-2} S cm^{-1}, while the conductivity of the acrylic film was 9.2×10^{-13}. By regarding the PAni content as 6.24 wt% in the AcPA nanocomposite, its electrical conductivity was interestingly high. In other words, the observed conductivity of the resulting nanocomposite film was much higher than the reported values for the nanocomposites prepared by interfacial polymerization with the same content of PAni [28, 30]. The high electrical conductivity observed was attributed to the presence of the ultralong PAni nanofibers, which possibly acted as efficient electrically conductive pathways in the structure of the AcPA nanocomposite film [31].

Figure 6 shows the TGA thermographs of pure PAni, acrylic copolymer and AcPA nanocomposite. For PAni, there are three thermal degradation stages. During heating up to 120 °C, the weight losses were generated by the residual water presented in the PAni sample. Water molecules are able to occupy sites instead of dopants; however, the residual water cannot be regarded as moisture, because all the samples were dried before TGA measurements [32]. The weight loss in the range of 150–250 °C represents the dopant loss and degradation of the oligomers. The third weight loss starting at 400 °C can be related to the thermal degradation of the PAni molecule [23].

Thermal degradation of the acrylic copolymer proceeds in three steps of weight losses. The first step is initiated by breaking of head-to-head linkages (resulting from termination by the combination of radicals). The last two stages of weight loss correspond to the degradation initiated at the unsaturated ends and at the polymer backbones. The second degradation peak is mainly because of vinylidene ends in the acrylic polymer chains. However, because of the high molecular weight of the synthesized polymer, there were not so many vinylidene ends and the corresponding peak was not prominent [33]. On the other hand, as can be seen in Fig. 6, the AcPA nanocomposite
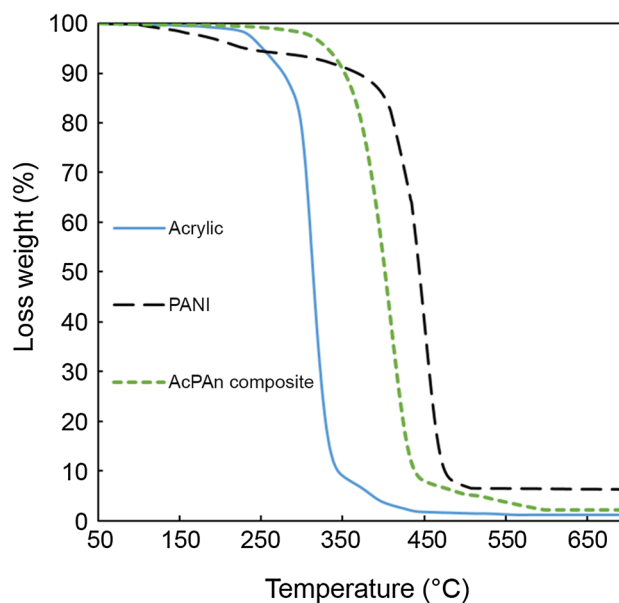
Fig. 6 TGA thermograms of PAni, acrylic copolymer and AcPA nanocomposite
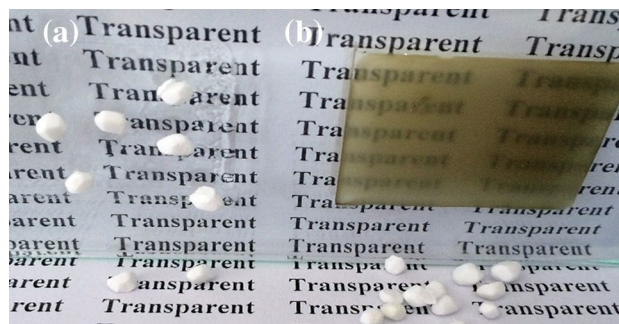
Fig. 7 Antistatic tests of **a** pure acrylic film and **b** AcPA nanocomposite film

shows better thermal stability compared to pure acrylic resin. In other words, the interactions between PAni and acrylic copolymer enhance the thermal stability of the acrylic copolymer [23].

In Fig. 7, the antistatic property of the pure transparent acrylic film (Fig. 7a) and the translucent conducting nanocomposite film (Fig. 7b) is compared. The two films are abraded and then placed between foamed polystyrene spheres. Clearly, the spheres are adsorbed on the surface of pure acrylic film, while they are not found on the AcPA nanocomposite film. This phenomenon indicates that the prepared nanocomposite film can efficiently act as an antistatic coating.

The mechanical properties of AcPA nanocomposite was investigated by a tensile test. The results are summarized in Table 1 for the acrylic and AcPA nanocomposite films. It is obvious that the AcPA nanocomposite possesses

Table 1 Mechanical properties of AcPA nanocomposite and acrylic copolymer films

Sample	Stress at yield (MPa)	Stress at break (MPa)	Strain at break (%)	Elongation at break (mm)	Tensile modulus (MPa)	Break work (MPa)
Acrylic	2.83	10.03	211.33	52.37	369.37	1923
AcPA nanocomposite	2.06	8.73	197.46	33.47	387.63	1537

inferior flexibility compared to the acrylic copolymer film. The decreased elasticity and increased modulus in the films were attributed to the presence of rigid phenyl ring in the anion structure of the doping acid [23]. However, the mechanical properties of AcPA nanocomposite are in a suitable range for its use as an antistatic coating.

Conclusion

A feasible and novel route to prepare waterborne antistatic organic coating has been successfully developed. A conducting composite made of emulsion-polymerized poly(MMA-BA-AA)/PAni was obtained using a process consisting of two stages: in the first step, the acrylic latex was obtained after the introduction of PAni into the latex through interfacial polymerization of aniline [(organic phase = chloroform + aniline)/(aqueous phase = acrylic latex + HCl + APS)]. The studies by FTIR and UV–Vis indicated that the prepared nanocomposite included emeraldine salt of PAni. Also, elemental analysis studies confirmed PAni loading of 6.24 wt% in the conducting nanocomposite structure. According to SEM results, the PAni nanofibers in the nanocomposite structure showed the diameter in the range of 0.078–1 μm and length around 12–67 μm which was higher than the reported length for PAni nanofibers prepared by interfacial polymerization method so far. The prepared nanocomposite showed an electrical conductivity of about 0.025 S/cm, which was several orders of magnitude higher than the electrical conductivity of the acrylic latex film (9.2×10^{-13} S/cm). TG analysis suggested that the thermal stability of the AcPA composite was higher than that of the pure acrylic copolymer, attributed to the interaction between PAni and the acrylic matrix. The resulting AcPA film exhibited good mechanical properties with a tensile modulus of 387.63 MPa and stress at break of 10.03 MPa. In summary, this work provided a straightforward method to prepare flexible conductive films with reasonable conductivity and good mechanical properties applicable as antistatic coating.

References

1. Coyard H, Oldring PK, Deligny P, Tuck N (2001) Resins for surface coatings: acrylics and epoxies. Wiley, New York
2. Sangermano M, Foix D, Kortaberria G, Messori M (2013) Multifunctional antistatic and scratch resistant UV-cured acrylic coatings. Prog Org Coat 76:1191–1196
3. Roessler A, Schottenberger H (2014) Antistatic coatings for wood-floorings by imidazolium salt-based ionic liquids. Prog Org Coat 77:579–582
4. Baughman RH, Zakhidov AA, de Heer WA (2002) Carbon nanotubes: the route toward applications. Science 297:787–792
5. Soto-Oviedo MA, Araújo OA, Faez R, Rezende MC, De Paoli MA (2006) Antistatic coating and electromagnetic shielding properties of a hybrid material based on polyaniline/organoclay nanocomposite and EPDM rubber. Synth Met 156:1249–1255
6. Guntermann U, Elschner A, Kirchmeyer S (2015) Conductive polymer layer as an antistatic protection shield for polarization filter. US Patent 20150064449 A1
7. Ansari SP, Mohammad F (2016) Conducting nanocomposites of polyaniline/nylon 6,6/zinc oxide nanoparticles: preparation, characterization and electrical conductivity studies. Iran Polym J 25:363–371
8. Ćirić-Marjanović G (2013) Recent advances in polyaniline research: polymerization mechanisms, structural aspects, properties and applications. Synth Met 177:1–47
9. Mostafaei A, Nasirpouri F (2014) Epoxy/polyaniline–ZnO nanorods hybrid nanocomposite coatings: synthesis, characterization and corrosion protection performance of conducting paints. Prog Org Coat 77:146–159
10. Navarchian AH, Joulazadeh F, Karimi F (2014) Investigation of corrosion protection performance of epoxy coatings modified by polyaniline/clay nanocomposites on steel surfaces. Prog Org Coat 77:347–353
11. Dhawan SK, Singh N, Rodrigues D (2003) Electromagnetic shielding behaviour of conducting polyaniline composites. Sci Technol Adv Mater 4:105–113
12. Sapurina I, Stejskal J, Špírková M, Kotek J, Prokeš J (2005) Polyurethane latex modified with polyaniline. Synth Met 151:93–99
13. Lee SM, Lee SJ, Kim JH, Cheong IW (2011) Synthesis of polystyrene/polythiophene core/shell nanoparticles by dual initiation. Polymer 52:4227–4234
14. Borthakur LJ, Konwer S, Das R, Dolui SK (2011) Preparation of conducting composite particles of styrene–methyl acrylate copolymer as the core and graphite-incorporated polypyrrole as the shell by surfactant-free miniemulsion polymerization. J Polym Res 18:1207–1215
15. Yang F, Zhu A (2015) Preparation and characterization of polyaniline-poly (styrene-acrylate) composite latexes. Polym Bull 72:2503–2518
16. Huijs F, Vercauteren F, Hadziioannou G (2001) Resistance of transparent latex films based on acrylic latexes encapsulated with a polypyrrole shell. Synth Met 125:395–400

17. Li R, Chen Z, Li J, Zhang C, Guo Q (2013) Effective synthesis to control the growth of polyaniline nanofibers by interfacial polymerization. Synth Met 171:39–44

18. Huang J, Kaner RB (2004) A general chemical route to polyaniline nanofibers. J Am Chem Soc 126:851–855

19. Olad A, Barati M, Shirmohammadi H (2011) Conductivity and anti-corrosion performance of polyaniline/zinc composites: investigation of zinc particle size and distribution effect. Prog Org Coat 72:599–604

20. Gharieh A, Mahdavian AR, Salehi-Mobarakeh H (2014) Preparation of core–shell impact modifier particles for PVC with nanometric shell thickness through seeded emulsion polymerization. Iran Polym J 23:27–35

21. Tripathi AK, Sundberg DC (2013) Partitioning of functional monomers in emulsion polymerization: distribution of carboxylic acid monomers between water and multimonomer systems. Ind Eng Chem Res 52:9763–9769

22. Huang J, Virji S, Weiller BH, Kaner RB (2003) Polyaniline nanofibers: facile synthesis and chemical sensors. J Am Chem Soc 125:314–315

23. Chen CH, Kan YT, Mao CF, Liao WT, Hsieh CD (2013) Fabrication and characterization of water-based polyurethane/polyaniline conducting blend films. Surf Coat Technol 231:71–76

24. Trchová M, Šeděnková I, Tobolková E, Stejskal J (2004) FTIR spectroscopic and conductivity study of the thermal degradation of polyaniline films. Polym Degrad Stab 86:179–185

25. Chen SA, Fang WG (1991) Electrically conductive polyaniline-poly (vinyl alcohol) composite films: physical properties and morphological structures. Macromolecules 24:1242–1248

26. Jin Y, Huang S, Zhang M, Jia M (2013) Preparation of sulfonated graphene–polyaniline nanofiber composites by oil/water interfacial polymerization and their application for supercapacitors. Synth Met 168:58–64

27. Chen CH, Dai YF (2011) Effect of chitosan on interfacial polymerization of aniline. Carbohydr Polym 84:840–843

28. Dai T, Qing X, Wang J, Shen C, Lu Y (2010) Interfacial polymerization to high-quality polyacrylamide/polyaniline composite hydrogels. Compos Sci Technol 70:498–503

29. Guan H, Fan LZ, Zhang H, Qu X (2010) Polyaniline nanofibers obtained by interfacial polymerization for high-rate supercapacitors. Electrochim Acta 56:964–968

30. Dallas P, Georgakilas V (2015) Interfacial polymerization of conductive polymers: generation of polymeric nanostructures in a 2-D space. Adv Colloid Interface Sci 224:46–61

31. Yu H, Chen P, Chen W, Liu Y (2014) Effect of cellulose nanofibers on induced polymerization of aniline and formation of nanostructured conducting composite. Cellulose 21:1757–1767

32. Plesu N, Ilia G, Pascariu A, Vlase G (2006) Preparation, degradation of polyaniline doped with organic phosphorus acids and corrosion essays of polyaniline–acrylic blends. Synth Met 156:230–238

33. Rahim-Abadi MM, Mahdavian AR, Gharieh A, Salehi-Mobarakeh H (2015) Chemical modification of TiO₂ nanoparticles as an effective way for encapsulation in polyacrylic shell via emulsion polymerization. Prog Org Coat 88:310–315